Journal of Cerebral Blood Flow & Metabolism (2010) 30, 1394–1402

www.jcbfm.com

Reorganization of gap junctions after focused ultrasound blood–brain barrier opening in the rat brain

Angelika Alonso[1], Eileen Reinz[2], Jürgen W Jenne[1], Marc Fatar[1], Hannah Schmidt-Glenewinkel[2], Michael G Hennerici[1] and Stephen Meairs[1]

[1]*Department of Neurology, Universitätsklinikum Mannheim, University of Heidelberg, Mannheim, Germany;* [2]*German Cancer Research Center, Im Neuenheimer Feld 280, Heidelberg, Germany*

Ultrasound-induced opening of the blood–brain barrier (BBB) is an emerging technique for targeted drug delivery to the central nervous system. Gap junctions allow transfer of information between adjacent cells and are responsible for tissue homeostasis. We examined the effect of ultrasound-induced BBB opening on the structure of gap junctions in cortical neurons, expressing Connexin 36, and astrocytes, expressing Connexin 43, after focused 1-MHz ultrasound exposure at 1.25 MPa of one hemisphere together with intravenous microbubble (Optison, Oslo, Norway) application. Quantification of immunofluorescence signals revealed that, compared with noninsonicated hemispheres, small-sized Connexin 43 and 36 gap-junctional plaques were markedly reduced in areas with BBB breakdown after 3 to 6 hours ($34.02 \pm 6.04\%$ versus $66.49 \pm 2.16\%$, $P = 0.02$ for Connexin 43; $33.80 \pm 1.24\%$ versus $36.77 \pm 3.43\%$, $P = 0.07$ for Connexin 36). Complementing this finding, we found significant increases in large-sized gap-junctional plaques ($5.76 \pm 0.96\%$ versus $1.02 \pm 0.84\%$, $P = 0.05$ for Connexin 43; $5.62 \pm 0.22\%$ versus $4.65 \pm 0.80\%$, $P = 0.02$ for Connexin 36). This effect was reversible at 24 hours after ultrasound exposure. Western blot analyses did not show any change in the total connexin amount. These results indicate that ultrasound-induced BBB opening leads to a reorganization of gap-junctional plaques in both neurons and astrocytes. The plaque-size increase may be a cellular response to imbalances in extracellular homeostasis after BBB leakage.
Journal of Cerebral Blood Flow & Metabolism (2010) **30,** 1394–1402; doi:10.1038/jcbfm.2010.41; published online 24 March 2010

Keywords: blood–brain barrier; Connexin 36; Connexin 43; gap junctions; microbubbles; ultrasound

Introduction

The blood–brain barrier (BBB) is a significant obstacle for delivery of therapeutic drugs to the brain. Indeed, both small molecules and macromolecular agents potentially useful for the treatment of neurologic diseases do not penetrate the intact BBB (Pardridge, 2005; Meairs and Alonso, 2007). Experimental studies indicate that ultrasound might be useful for local delivery of drugs to the brain because of its ability to transiently open the BBB (Hynynen *et al*, 2001; McDannold *et al*, 2005). The effect of BBB opening by ultrasound is accentuated in the presence of gas-filled microbubbles, thus allowing a reduction in acoustic pressure along with a more focused energy delivery to blood vessels. In the presence of microbubbles, pulsed ultrasound is able to transiently open the BBB without neuronal damage (Hynynen *et al*, 2001). However, depending on the level and duration of acoustic pressures (Hynynen *et al*, 2005), as well on as the concentration and physical/chemical properties of microbubbles for BBB opening (Treat *et al*, 2007), variable neuronal and glial cell damage can occur.

The integrity of the neuronal network depends on an intact intercellular communication mediated by gap junctions. These channel-forming structures in contacting plasma membranes have pores allowing the exchange of molecules such as ionic currents or second messengers. Gap junctions function as electrical synapses and can synchronize large cellular ensembles. They further may subserve metabolic

Correspondence: Dr A Alonso, Department of Neurology, Universitätsmedizin Mannheim, University of Heidelberg, Theodor-Kutzer-Ufer 1-3, 68167 Mannheim, Germany.
E-mail: alonso@neuro.ma.uni-heidelberg.de
The research leading to these results has received funding from the European Union's Seventh Framework Programme (FP7/2007-2013) under grant agreements no. 201024 and no. 202213 (European Stroke Network).
Received 10 November 2009; revised 18 January 2010; accepted 25 February 2010; published online 24 March 2010

coupling and chemical communication (for a recent review, see Sohl *et al*, 2005). Gap junctions are formed by two hemichannels built up by six transmembrane proteins termed connexins. The connexin proteins are encoded by a gene family of at least 20 members in mammals, with differing cellular specifity. Connexin 36 is the principal connexin expressed in neurons (Condorelli *et al*, 1998), together with a site-specific expression of Connexins 45 and 57. Astrocytic gap junctions are mainly characterized by Connexin 43 expression (Yamamoto *et al*, 1990). When coupled cells are subjected to stress or injury, both deleterious and health-promoting molecules may spread on neighboring cells through gap-junctional coupling. Depending on the balance, this may lead to bystander killing with propagation of damage or rescue of neighboring cells and tissue (for a review, see Contreras *et al*, 2004). Modulation of gap-junctional coupling after noxa-like ischemic stress has been shown to occur in terms of upregulation of connexin expression (Oguro *et al*, 2001). The functional significance of changes in connexin expression yet remains unresolved. However, they may be attributed to adaptive processes to tissue damage and may contribute to cell survival and resistance.

In this study, we examined the gap-junctional integrity in rat brains after ultrasonic insonation. Connexin 43 and 36 protein expressions were examined at different time points after ultrasound exposure to investigate the biologic effects of ultrasound parameters useful for nondestructive BBB opening on gap-junctional coupling.

Materials and methods

Animals

All experiments were approved by the local government authorities in accordance with the animal protection guidelines. In all, 16 male Wistar rats weighing 360 to 430 g were anesthetisizedanesthetized with 1.5% isofluorane. Body temperature was regulated with a heating pad. The hair over the skull was removed with an electric shaver and depilatory cream, and the tail vein was catheterized with a 24-G Itrocan Safety IV Catheter (Braun, Melsungen, Germany).

Ultrasound Device

The ultrasound field was generated by an air-backed piezoelectric transducer disc (30 mm diameter, SST Sensor & Transducer Technology, Mühlanger, Germany) with a center frequency of 1 MHz. The ultrasound field was focused with a lens of polystyrol (focal length 41.6 mm). The elliptical shaped −6 dB focus had a length of 1.1 mm and a diameter of 20.8 mm. The transducer was driven by a function generator (Agilent 33120 A Function/Arbitrary Waveform Generator, Agilent Technologies, Santa Clara, CA, USA) feeding an RF-amplifier (model 40AD1, AR Amplifier Research, Souderton, PA, USA). The pressure amplitude was set to 2.5 MPa as assessed by a calibrated 400 μm diameter hydrophone (HGL 400 Onda Corporation, Sunnyvale, CA, USA) in water. As the attenuation of the ultrasound wave passing the intact skull bone is 49% (Treat *et al*, 2007), the actual intracranial pressure amplitude is $\sim$1.25 MPa. This corresponds to previously reported ultrasound parameters chosen for BBB opening in the rat brain through an intact rat skull (Treat *et al*, 2007). The length of the ultrasound pulses was set to 10 ms at a repetition frequency of 1 Hz. Insonation time was 1 minute.

Experimental Setup

The transducer was submerged and fixed in a tank of deionized water. Rats were placed supine on a sheet with a heating pad with the skull immersed into the water tank. The center of the ultrasound focus was aimed to the middle of the rat brain. One hemisphere was insonicated, whereas the contralateral hemisphere was used as an intraindividual control. Through the tail vein catheter, rats received perflutren microbubbles at a dosage of 0.1 mL/kg body weight (Optison, Amersham Health AS, Oslo, Norway). Insonation was started together with microbubble injection. Insonations without microbubble application were not performed as previous studies have showed that much higher pressure amplitudes with subsequent cell and tissue damage are required (Hynynen *et al*, 2001). After insonation, a 2% solution of Evans Blue (molecular weight 960.82 Da) at a dosage of 4 mL/kg body weight was slowly infused intravenously to provide macro- and microscopic verification of focal opening of the BBB.

A total of 16 animals were treated and included in the final analyses. There were no drop outs. All animals were killed in deep anesthesia by transcardial perfusion with 2% paraformaldehyde and 0.5% glutaraldehyde at the following time points: 0.5 hour ($n=3$), 1 hour ($n=4$), 3 hours ($n=4$), 6 hours ($n=3$), and 24 hours ($n=2$). The brains were removed, cryofixed in ice-cold isopentane, and stored at −80°C.

Immunohistochemistry

Coronal sections were cut at 10 μm on a freezing microtome (Leica CM 1900, Bensheim, Germany) and treated with 10 mmol/L Tris–HCl at 98°C for demasking. Endogenous peroxidase was blocked with TBST containing 5% bovine serum. Primary antibodies against Connexin 43 (anti-Connexin 43, ZYMED Laboratories, Karlsruhe, Germany; Rabbit, 71-0700), phosphorylated Connexin 43 (antiphosphorylated Connexin 43 (8S279/S282); Leykauf *et al*, 2006), and Connexin 36 (anti-Connexin 36, ZYMED Laboratories, Rabbit, 36-4600) were used in TBST containing 5% bovine serum. Immunoreaction was visualized using the DAKO EnVision + System, Peroxidase kit (Dako, Carpinteria, CA, USA): Sections were incubated with peroxidase-labeled polymer followed by incubation in 3,3′-diaminobenzidine (DAB) + substrate-chromogen.

Immunofluorescence

In all, 10 μm cryosections were treated with TBS-Triton X-100 0.2% and later incubated with primary antibodies

against Connexin 43 (1:100), Connexin 36 (1:50), and albumin (antirat albumin, sheep, FITC-labeled, AbD Serotec 0220-2424F; 1:100) overnight. After washing in TBS-Triton X-100 0.2%, sections were incubated with a donkey antirabbit antibody coupled to Alexa Fluor 488 (A11034, Invitrogen, Karlsruhe, Germany; 1:800) or a goat antirabbit antibody coupled to Alexa Fluor 594 (A11011, Invitrogen; 1:800). Later, sections were again washed and mounted in antifading medium. Images were taken with a confocal microscope (Leica DM IRBE).

Immunoblotting

For immunoblotting, rats were treated with ultrasound as described and the brain snap-frozen in liquid nitrogen. Thin slices containing exclusively Evans Blue-positive material from the sonicated hemisphere and material from the nonsonicated hemisphere were excised and homogenized in a cell disruptor and taken in buffer X (Pierce, Bonn, Germany). Proteins from both hemispheres (15 μg) were separated on gradient acrylamide gels, blotted onto polyvinylidenefluoride (PVDF) membranes, and incubated with antibodies to Connexin 43. Reacting bands were revealed by enhanced chemiluminiscence (G&E, Freiburg, Germany). Bands were quantified using the QuantTL computer program.

Quantification of Connexins in Confocal Images

Confocal images from double immunofluorescence experiments were used for quantification. The presence of albumin indicated BBB opening. Plaques from at least 1,000 cells per time point were quantified using the image processing package ImageJ (National Institute of Health, Betheseda, MD, USA). Image segmentation involved use of a median filter with thresholding to create a binary image. Extraction of morphometric features including vesicle size, location, intensity, and colocalization of immunofluorescence was performed with the 'analyze particles' function of ImageJ (Dibaj *et al*, 2007). Filter and threshold parameters were held constant for all images analyzed. For the detection of *P*-values, a one-sided *t*-test was performed ($^{**}P<0.05$; $^{***}P<0.01$).

Results

Opening of the Blood–Brain Barrier

The disruption of the BBB was documented by Evans Blue extravasation. Macroscopically, the outer surface of the insonicated hemispheres showed a focal blue staining as depicted in Figure 1A, whereas nontreated hemispheres showed no blue stain. Visual inspection of the 2- to 3-mm-thick sections revealed a penetration of blue dye throughout the whole underlying cortex (Figures 1B and 1C).

To further substantiate these results, microscopic data were obtained by detection of albumin leakage with antibodies to rat albumin labeled with FITC (see Supplementary Figure 2). Albumin immunoreactivity was most intense in perivascular areas of the insonicated hemisphere. However, strong and widespread albumin extravasation was also found throughout the cortical brain parenchyma, as shown in Figure 1D. No immunoreaction products were detected in the nontreated hemispheres, as shown in Figure 1E.

Prussian blue staining of histologic samples at all time points for detection of Fe3 showed only a very limited number of blue-stained cells restricted to

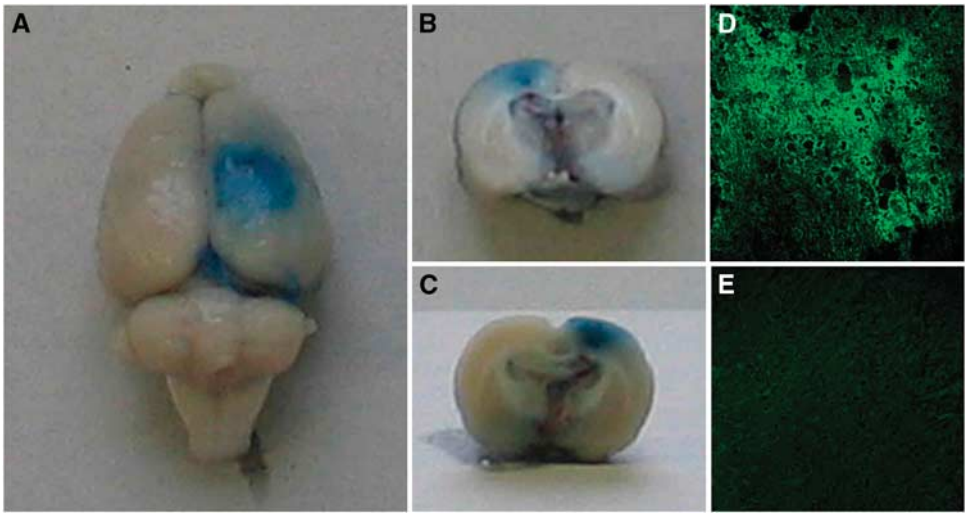

Figure 1 Detection of blood–brain barrier (BBB) opening. The right hemisphere was insonicated at an intracranial pressure amplitude of 1.25 MPa in the presence of microbubbles at a dosage of 0.1 mL/kg. Macroscopic inspection of the brain surface immediately after killing showed a circular extravasation of Evans Blue dye (**A**); 2 to 3 mm thick coronal sections showed penetration of Evans Blue into the underlying cortex (**B**, front side; **C**, reverse side). Immunofluorescence with detection of extravasated albumin confirmed this finding. Confluent and widespread albumin-positive reaction products were found in the brain parenchyma of insonicated hemispheres (**D**), whereas no albumin extravasation was observed in the nontreated left hemisphere (**E**). Magnification in (**D**, **E**) $\times 200$.

submeningeal regions. This finding indicates that no relevant hemorrhage occurred after insonation (see Supplementary Figure 1).

Expression of Connexin 36 in the Cortex of Ultrasound-Treated Rats

To evaluate alterations in Connexin 36 expression in the cortex after insonation, histochemical analyses of ultrasound-treated versus nontreated hemispheres were performed. As shown in Figure 2B, no major differences in Connexin 36 expression could be detected immunohistochemically in cortical areas of insonicated hemispheres (Figure 2B left) as compared with intact cortical areas (Figure 2B right) 6 hours after insonation.

To further substantiate these results, immunofluorescence experiments were performed. At high magnification, irregular punctate to more particulate structures were visible. These punctate structures were mainly localized at the cellular membranes, but some of them were also found with intracellular location. The general Connexin 36 staining pattern was similar in both areas with or without albumin leakage as depicted in Figures 2A and 2C. This was true for animals killed 0.5 to 24 hours after insonation. However, Connexin 36-positive plaques appeared to be somewhat coarser and more intense in areas with BBB breakdown 3 and 6 hours after insonation (Figures 2A and 2C).

Computerized quantification of the structures confirmed this observation. In animals killed 1 hour after insonation, the plaque-size distribution did not differ between albumin-positive and albumin-negative areas (Figure 3A). However, we could show a statistically significant shift to larger plaques (small-sized plaques $33.80 \pm 1.24\%$ versus $36.77 \pm 3.43\%$ in control hemispheres, $P = 0.07$; large-sized plaques $5.62 \pm 0.22\%$ versus $4.65 \pm 0.80\%$ in control hemi-

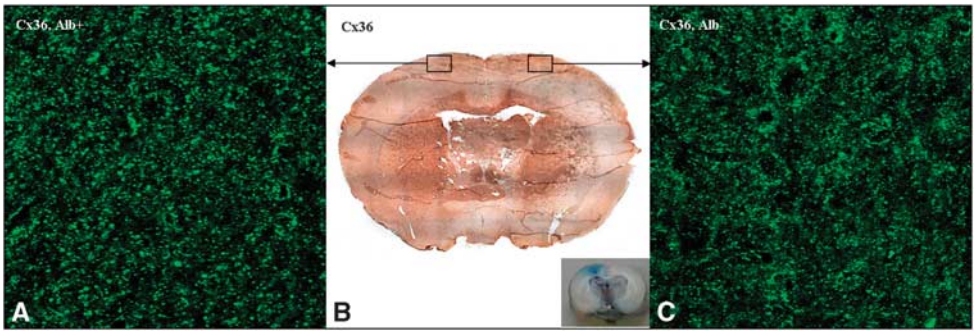

Figure 2 Immunofluorescence and immunohistochemistry with detection of Connexin (Cx) 36. Immunohistochemistry with antibodies against Cx 36 (**B**) showed no overall differences in Cx 36 expression patterns of insonicated (right hemisphere, see the inset) compared with control hemispheres (left hemisphere, see the inset) 6 hours after ultrasound-induced blood–brain barrier (BBB) opening. In immunofluorescence experiments, both hemispheres revealed an irregular punctate staining pattern (**A**, **C**). However, immunoreactivity appeared to be increased in areas with BBB leakage (**A**), with a denser and more particulate staining pattern compared with areas with intact BBB (**C**). Magnification in (**A**, **C**) $\times 630$. Alb+, albumin-positive area; Alb−, albumin-negative area.

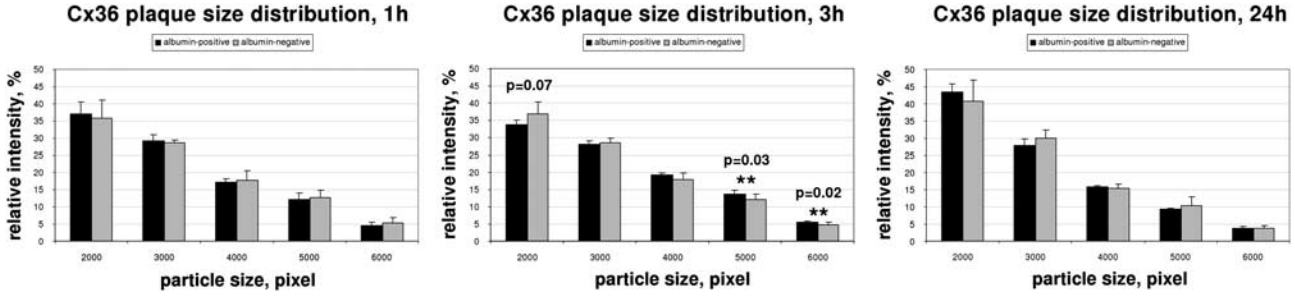

Figure 3 Quantification of immunofluorescence signals for Connexin (Cx) 36. For quantification, confocal pictures from double immunofluorescence were taken. Regions of the insonicated hemispheres were analyzed by taking the presence of albumin as proof for blood–brain barrier (BBB) opening. Regions of the noninsonicated, albumin-negative hemisphere were considered to have an intact BBB. Connexin immunosignals were quantified from segmented images. Vesicle sizes of immunosignals can be correlated to gap-junctional plaque size; 1 hour after sonication, vesicle sizes of Cx 36 immunoreactivity in areas with BBB breakdown (albumin-positive) and control areas (albumin-negative) did not differ, with a prevalence of small-sized plaques in both samples. Three hours after ultrasound-induced BBB opening, a significant shift toward larger-sized plaques was observed in areas with albumin leakage. This effect was completely reversible after 24 hours. Black bars, albumin-positive; gray bars, albumin-negative.

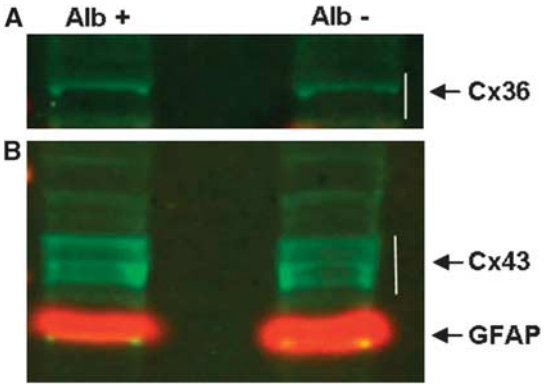

Figure 4 Western blot analyses of Connexin (Cx) 36 (**A**) and Cx 43 (**B**) in areas with blood–brain barrier (BBB) breakdown (left slot; Alb +, albumin-positive area) and control hemispheres (right slot, Alb−, albumin-negative area). Specific reacting bands for Cx 36 were found in samples of both insonicated and control hemispheres, but no significant differences between hemispheres in band densities were observed 24 hours after ultrasound-induced BBB opening. Immunoblots of Cx 43 revealed three protein bands in the range of 43 to 48 kDa, correlating to unphosphorylated, phosphorylated, and hyperphosphorylated Cx 43, respectively (**B**). No significant differences in signal intensity between homogenates of insonicated versus control areas could be observed. GFAP, glial fibrillary acidic protein, marker protein at 55 kDa.

spheres, $P = 0.02$) in areas with albumin leakage when analyzing animals 3 hours after ultrasound treatment (Figure 3B). This effect persisted at 6 hours after insonation and was found to be reversible after 24 hours (Figure 3C).

To evaluate whether these changes can be exclusively affiliated to reallocation or whether they are associated with upregulation of Connexin 36 expression, we performed western blot analyses (Figure 4A). Immunoblots with anti-Connexin 36 resulted in detection of protein bands between the 34- and 49-kDa marker bands corresponding to Connexin 36 in homogenates of both ultrasound-treated and nontreated hemispheres 6 hours after insonation. Quantification of the reacting bands with QuantTL showed no difference in total Connexin 36 levels, indicating that no upregulation of Connexin 36 expression had occurred.

Expression of Connexin 43 and Phosphorylated Connexin 43 in the Cortex of Ultrasound-Treated Rats

To investigate changes in astrocytic gap junctions after insonation, immunohistochemical analyses were performed. Similar to our findings for Connexin 36, we could not observe any general changes in histochemical staining patterns after ultrasound treatment (data not shown). In our subsequently performed immunofluorescence experiments, the immunostaining pattern of Connexin 43 in the rat cortex confirmed previous results (Yamamoto *et al*, 1990). Immunoreactivity was found in the form of irregular punctate to more particulate reaction products along cellular membranes and to a smaller amount within the cytoplasm of cells. Around blood vessels, immunopositive reaction products formed linear to reticular structures. Again, the distribution and staining pattern of Connexin 43 was found to be in general preserved in the cortex of ultrasound-treated hemispheres up to 24 hours after insonation (Figures 5A and 5B). Taking into consideration Connexin 43's half-life of a few hours in adult rats (Saez *et al*, 2003), a complete turnover of Connexin 43 within 24 hours can be assumed for this time point; larger time intervals were therefore not analyzed. Similar to our observations for Connexin 36, Connexin 43 reacting plaques tended to be coarser grained in animals killed 3 and 6 hours after insonation. This observation held true for both perivascular and parenchymal areas with BBB disruption.

Computerized analyses of plaque-size distribution could verify this effect. Six hours after insonation, vesicle quantification revealed a significant decrease in small-sized plaques ($34.02 \pm 6.04\%$ versus $66.49 \pm 2.16\%$ in control hemispheres, $P = 0.02$), together with a significant increase in larger plaques ($5.76 \pm 0.96\%$ versus $1.02 \pm 0.84\%$ in control hemispheres, $P = 0.05$), in ultrasound-treated hemispheres (Figure 6A).

To assess the total amount of protein levels, we performed immunoblotting with anti-Connexin 43 of the homogenates of insonicated and control hemispheres. In both the samples, three protein bands in the range of 43 to 48 kDa could be detected, correlating to unphosphorylated, phosphorylated, and hyperphosphorylated Connexin 43, respectively. Computerized quantification of the reacting bands did not show any difference in total Connexin 43 amount between insonicated and nontreated hemispheres (Figure 4B). Thus, our results show that changes in Connexin 43 are rather attributable to reassembly than to upregulation.

It has been shown that Connexin 43 phosphorylation is related to protein degradation. For this reason, we analyzed the phosphorylation stage of Connexin 43 after ultrasound treatment using an antibody specific for S279/S282 phosphorylation. We found that expression of phosphorylated Connexin 43 was restricted to the endothelial cells of blood vessels in which a linear to reticular staining pattern was observed at high magnifications. Cellular membranes or the cytoplasm of glial cells in the brain parenchyma did not stain positive for the phosphorylated isoform of Connexin 43. This staining pattern was not altered in ultrasound-treated hemispheres over the time course of 24 hours, as shown in Figures 5D and 5E. Complementarily to the data from the immunofluorescence experiments, western blot analyses showed steady-state protein levels of phosphorylated Connexin 43 after ultrasound treatment as mentioned above. The results indicate that

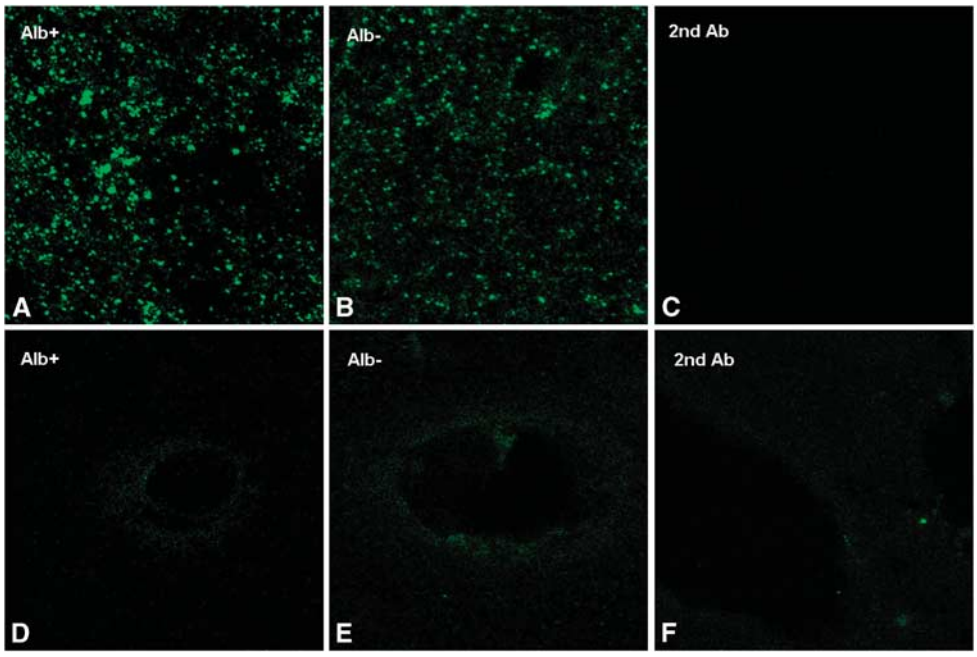

Figure 5 Immunofluorescence of Connexin (Cx) 43 and phosphorylated Cx 43. Three hours after ultrasound-induced opening of the blood–brain barrier (BBB), no major differences in the total amount of stained connexin between albumin-positive and albumin-negative could be observed (**A**, Alb + , albumin-positive; **B**; Alb−, albumin-negative areas). Both hemispheres exhibited a punctate to particulate Cx 43 staining pattern, which, however, appeared to be somewhat denser in areas with BBB breakdown (**A**). (**C**) Negative control without primary antibody. The phosphorylated Cx 43 isoform was restricted to blood vessels. Three hours after insonation, a linear to reticulate staining pattern was observed both in sonicated (**D**; Alb + , albumin-positive areas) and control hemispheres (**E**; Alb−, albumin-negative areas). (**F**) Negative control without primary antibody without any apparent differences.

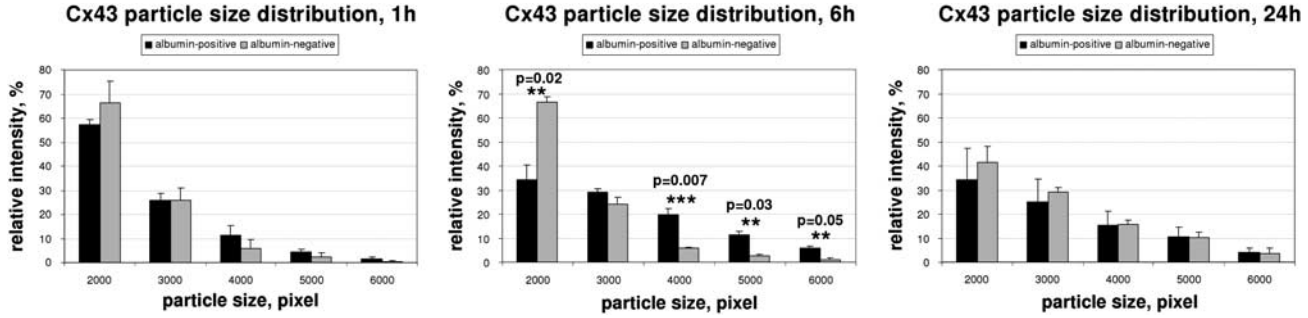

Figure 6 Quantification of immunofluorescence signals for Connexin (Cx) 43. As described in Figure 3, confocal pictures from double immunofluorescence were taken and connexin immunosignals were quantified from segmented images. Quantification of vesicle sizes of Cx 43 immunoreactivity signals revealed a significant shift toward larger size plaques 6 hours after ultrasound treatment in insonicated areas compared with control hemispheres. Small-sized plaques were found to be significantly reduced in insonicated areas after 6 hours. As for Cx 36, this effect disappeared after 24 hours. Black bars, albumin-positive; gray bars, albumin-negative.

phosphorylation of Connexin 43 is not influenced by insonation for BBB opening.

Discussion

Focused ultrasound can be used for noninvasive and focal disruption of the BBB, thus providing a unique opportunity for targeted drug or gene delivery to the brain. Severe cell and tissue damage can be avoided by application of appropriate insonation parameters. However, there has been no information so far on alterations in intercellular communication mediated by gap junctions in surviving cells. Our study now shows that (i) ultrasound for BBB opening does not lead to destruction or loss of gap-junctional plaques, (ii) ultrasound can induce reversible changes in gap-junctional plaque assembly in both neurons and astrocytes, and (iii) these changes are not attended by an upregulation of connexin protein levels.

Electrical coupling between central nervous system cells occurs through neuronal (Sohl *et al*, 2005) and astrocytic (Nagy *et al*, 2004) gap junctions. Recent studies provide evidence that electrical synapses may occur also between neurons and glia, at least in some restricted regions (Alvarez-Maubecin *et al*, 2000). We performed immunohistochemistry, immunofluorescence, and western blot analyses of Connexins 36 and 43. Through our histochemical and immunofluorescence experiments, we could show that insonation of the rat cortex does not result in gap-junctional destruction over a time period of 24 hours after ultrasound treatment, as a preserved staining pattern was found for both neuronal and astrocytic gap junctions. Taking into consideration the short half-life of connexins of a few hours (Leykauf *et al*, 2006), we can assume that a more than complete connexin turnover occurred after this time period. Thus, direct adverse effects with loss of gap junctions at a later time are not expected.

Further, our results show no changes in the phosphorylation pattern of Connexin 43 when using an antibody specific for S279/S282 phosphorylation (Leykauf *et al*, 2003). As connexin phosphorylation of both amino acids has been correlated with increased degradation (Laird, 2005; Lampe and Lau, 2004; Leykauf *et al*, 2006), these results support our immunofluorescence findings and indicate that opening of the BBB with ultrasound does not result in increased connexin degradation.

Analyses of plaque-size distribution in immunofluorescence demonstrated a significant shift from smaller-sized to larger Connexin 36 and 43 immunopositive reaction products in the cortex of insonicated hemispheres. This effect was ascertained as soon as 3 hours after ultrasound treatment, persisted up to 6 hours after insonation, and was found to be reversible after 24 hours. In contrast, we found no evidence for an increment in Connexin 36 or Connexin 43 protein abundance as examined by western blot analyses. These results suggest that changes in Connexins 36 and 43 may be attributable to redistribution processes rather than to an upregulation of connexins. Considering a particle size shift toward larger vesicles, we postulate that the observed changes are attributable to the formation of larger gap-junctional plaques at the plasma membrane.

Role of Connexin 43

A reorganization of Connexin 43 in astrocytic gap junctions without protein upregulation has also been described by Hossain *et al* (1994) as a response to global ischemia in the rat brain. Similar to our findings, an increased punctate Connexin 43 immunoreactivity was found in areas with mild to moderate damage 2 days after injury, whereas areas of reduced staining surrounded by elevated levels of Connexin 43 immunoreactivity were observed in regions with severe ischemic damage. The hypothesis of injury-induced redistribution of astrocytic Connexin 43 is further supported by Oguro *et al* (2001), who found no alteration in Connexin 43 protein levels from 8 hours to 7 days after global ischemia in mouse hippocampus. Somewhat divergently, Haupt *et al* (2007) reported elevated hybridization signals for Connexin 43 mRNA and increased immunostaing of Connexin 43 protein in the vicinity of the lesions after photothrombotic ischemic injury, suggesting a reactive upregulation of Connexin 43. However, these findings might also be explained by redistribution processes, as the Connexin 43 staining was reported to appear coarser after injury, similar to our results.

However, the regulatory mechanisms of Connexin 43 redistribution are not understood. It has been suggested that phosphorylation of Connexin 43 contributes to trafficking of newly synthesized protein, as well as to its organization into functional gap-junctional plaques (Musil *et al*, 1990). Nevertheless, we could not detect differences in phosphorylated Connexin 43 distribution or protein levels after insonation in either immunofluorescence or western blot analyses.

Recent work has highlighted a role for the zonula occludens-1 protein (ZO-1) in organization and regulation of gap-junctional plaque size (Hunter *et al*, 2005). ZO-1 has been shown to interact with the C-terminus of Connexin 43 (Toyofuku *et al*, 1998). Blockade of the Connexin 43 binding site leads to a significant increase in plaque size (Hunter *et al*, 2005). Sheikov *et al* (2008) found evidence for a reversible disintegration of the tight-junctional molecular complexes with a transient loss of immunosignals for ZO-1 after ultrasound-induced opening of the BBB. Consistent with our findings, changes in tight-junctional molecule expression appeared a few hours after insonation, with full restoration at 24 hours (Sheikov *et al*, 2008). Inhibition of Connexin 43/ZO-1 interaction because of transient disintegration of ZO-1 may thus be considered as a crucial mechanism in ultrasound-induced changes of gap-junctional plaques. From a functional perspective, increased plaque size has been correlated with the increasing percentage of open channels (O'Brien *et al*, 2006; Bukauskas *et al*, 2000). As astrocytes control extracellular ion concentrations, and coupling of astrocytes through gap junctions can facilitate potassium spatial buffering (Wallraff *et al*, 2006), an enhanced permeability of astrocytic gap junctions will probably lead to an increased buffer capacity. In the case of a BBB breakdown, this may provide neuroprotection from hyperexcitability because of paracellular leakage of ions and other agents, which can pervade with molecular weights up to at least 40 kDa (Sheikov *et al*, 2008).

Although changes in gap-junctional plaque size were evident within a few hours after ultrasound-induced BBB opening, Connexin 43 redistribution processes in ischemic damage have been reported to occur only several days after the injury (Oguro *et al*,

2001; Hossain *et al*, 1994; Haupt *et al*, 2007). Astrocytes are relatively insensitive to ischemia, possibly because of their ability to switch from aerobic to anaerobic metabolism (Peuchen *et al*, 1996). Astrocytic gap junctions, which remain functional, can thus mediate neuronal protection *inter alia* by spatial buffering of potassium and neuronal Ca^{2+} from dying neurons. More delayed effects are mediated by astrocytic production of neurotrophic factors and cytokines (Schwartz *et al*, 1994). Contradictory to these studies, astrocytic gap junctions have been shown to propagate cell damage in ischemic injury (Lin *et al*, 1998; Rami *et al*, 2001; Rawanduzy *et al*, 1997), potentially by propagation of calcium overload or oxidative stress. The protective or derogating effect of astrocytic coupling might therefore depend on the relation between astrocytic buffering capacity and the extent of deleterious signals or molecules.

Role of Connexin 36

In the adult rat brain cortex, gap-junctional coupling is predominantly found between γ-aminobutyric acid-containing interneurons, whereas electrical coupling between excitatory principal neurons has not been unequivocally measured (Fukuda and Kosaka, 2003; for a review, see Bennett and Zukin, 2004). Interneuronal coupling facilitates the generation of rhythmic oscillations (Gibson *et al*, 1999). Synchronous firing of interneurons produces well-correlated patterns of inhibition in pyramidal neurons. The contribution of Connexin 36 to interneuronal gap-junctional coupling has been investigated in Connexin 36 knockout mice. Deletion of Connexin 36 resulted in weak and restricted rhythmic oscillation, indicating that Connexin 36 is indispensable for the generation of widespread, synchronous inhibitory activity (Deans *et al*, 2001). After ultrasound-induced opening of the BBB, we could show a reorganization of Connexin 36-containing gap junctions with increase in gap-junctional plaque size. The early and simultaneous onset of changes in Connexins 36 and 43 indicates that (1) the changes might be induced by the same pathway, and (2) that this pathway may rather not include translational or transcriptional changes as further supported by the western blot analyses. In fact, Connexin 36 has been found to interact with a ZO-1 PDZ domain (Li *et al*, 2004), similar to Connexin 43, thus suggesting that ultrasound-induced disruption of ZO-1 might be the key trigger for increasing Connexin 36 plaque size. Comparable to our hypothesis on the role of astrocytic gap-junctional reorganization, Connexin 36 redistribution might be involved in a reinforced clearance of extracellular ion imbalances. A rapid restoration of the extracellular milieu could possibly be critical for preservation of the functional integrity of the large interneuronal networks. However, changes in Connexin 36 plaque size were not as striking as in astrocytic Connexin 43 plaques, possibly pointing to the major importance of astrocytes for the restoration of homeostasis.

In conclusion, our study provides evidence that ultrasound-induced opening of the BBB induces rapid and reversible reorganization of both astrocytic and neuronal gap-junctional plaques. This redistribution might be crucial for cell survival and resistance to disequilibration of the extracellular milieu after BBB disruption.

Conflict of interest

The authors declare no conflict of interest.

References

Alvarez-Maubecin V, Garcia-Hernandez F, Williams JT, Van Bockstaele EJ (2000) Functional coupling between neurons and glia. *J Neurosci* 20:4091–8

Bennett MV, Zukin RS (2004) Electrical coupling and neuronal synchronization in the mammalian brain. *Neuron* 41:495–511

Bukauskas FF, Jordan K, Bukauskiene A, Bennett MV, Lampe PD, Laird DW, Verselis VK (2000) Clustering of connexin 43-enhanced green fluorescent protein gap junction channels and functional coupling in living cells. *Proc Natl Acad Sci USA* 97:2556–61

Condorelli DF, Parenti R, Spinella F, Trovato SA, Belluardo N, Cardile V, Cicirata F (1998) Cloning of a new gap junction gene (Cx36) highly expressed in mammalian brain neurons. *Eur J Neurosci* 10:1202–8

Contreras JE, Sanchez HA, Veliz LP, Bukauskas FF, Bennett MV, Saez JC (2004) Role of connexin-based gap junction channels and hemichannels in ischemia-induced cell death in nervous tissue. *Brain Res Brain Res Rev* 47:290–303

Deans MR, Gibson JR, Sellitto C, Connors BW, Paul DL (2001) Synchronous activity of inhibitory networks in neocortex requires electrical synapses containing connexin36. *Neuron* 31:477–85

Dibaj P, Kaiser M, Hirrlinger J, Kirchhoffà F, Neusch C (2007) Kir4.1 channels regulate swelling of astroglial processes in experimental spinal cord edema. *J Neurochem* 103:2620–8

Fukuda T, Kosaka T (2003) Ultrastructural study of gap junctions between dendrites of parvalbumin-containing GABAergic neurons in various neocortical areas of the adult rat. *Neuroscience* 120:5–20

Gibson JR, Beierlein M, Connors BW (1999) Two networks of electrically coupled inhibitory neurons in neocortex. *Nature* 402:75–9

Haupt C, Witte OW, Frahm C (2007) Up-regulation of Connexin43 in the glial scar followingphotothrombotic ischemic injury. *Mol Cell Neurosci* 35:89–99

Hossain MZ, Peeling J, Sutherland GR, Hertzberg EL, Nagy JI (1994) Ischemia-induced cellular redistribution of the astrocytic gap junctional protein connexin43 in rat brain. *Brain Res* 652:311–22

Hunter AW, Barker RJ, Zhu C, Gourdie RG (2005) Zonula occludens-1 alters connexin43 gap junction size and organization by influencing channel accretion. *Mol Biol Cell* 16:5686–98

Hynynen K, McDannold N, Sheikov NA, Jolesz FA, Vykhodtseva N (2005) Local and reversible blood-brain barrier disruption by noninvasive focused ultrasound at frequencies suitable for trans-skull sonications. *Neuroimage* 24:12–20

Hynynen K, McDannold N, Vykhodtseva N, Jolesz FA (2001) Noninvasive MR imaging-guided focal opening of the blood-brain barrier in rabbits. *Radiology* 220:640–6

Laird DW (2005) Connexin phosphorylation asa regulatory event linked to gap junction internalization and degradation. *Biochim Biophys Acta* 1711:172–82

Lampe PD, Lau AF (2004) The effects of connexin phosphorylation on gap junctional communication. *Int J Biochem Cell Biol* 36:1171–86

Leykauf K, Durst M, Alonso A (2003) Phosphorylation and subcellular distribution of connexin43 in normal and stressed cells. *Cell Tissue Res* 311:23–30

Leykauf K, Salek M, Bomke J, Frech M, Lehmann WD, Durst M, Alonso A (2006) Ubiquitin protein ligase Nedd4 binds to connexin43 by a phosphorylation-modulated process. *J Cell Sci* 119:3634–42

Li X, Olson C, Lu S, Kamasawa N, Yasumura T, Rash JE, Nagy JI (2004) Neuronal connexin36 association with zonula occludens-1 protein (ZO-1) in mouse brain and interaction with the first PDZ domain of ZO-1. *Eur J Neurosci* 19:2132–46

Lin JH, Weigel H, Cotrina ML, Liu S, Bueno E, Hansen AJ, Hansen TW, Goldman S, Nedergaard M (1998) Gap-junction-mediated propagation and amplification of cell injury. *Nat Neurosci* 1:494–500

McDannold N, Vykhodtseva N, Raymond S, Jolesz FA, Hynynen K (2005) MRI-guided targeted blood-brain barrier disruption with focused ultrasound: histological findings in rabbits. *Ultrasound Med Biol* 31:1527–37

Meairs S, Alonso A (2007) Ultrasound, microbubbles and the blood-brain barrier. *Prog Biophys Mol Biol* 93:354–62

Musil LS, Cunningham BA, Edelman GM, Goodenough DA (1990) Differential phosphorylation of the gap junction protein connexin43 in junctional communication-competent and -deficient cell lines. *J Cell Biol* 111:2077–88

Nagy JI, Dudek FE, Rash JE (2004) Update on connexins and gap junctions in neurons and glia in the mammalian nervous system. *Brain Res Brain Res Rev* 47:191–215

O'Brien JJ, Li W, Pan F, Keung J, O'Brien J, Massey SC (2006) Coupling between A-type horizontal cells is mediated by connexin 50 gap junctions in the rabbit retina. *J Neurosci* 26:11624–36

Oguro K, Jover T, Tanaka H, Lin Y, Kojima T, Oguro N, Grooms SY, Bennett MV, Zukin RS (2001) Global ischemia-induced increases in the gap junctional proteins connexin 32 (Cx32) and Cx36 in hippocampus and enhanced vulnerability of Cx32 knock-out mice. *J Neurosci* 21:7534–42

Pardridge WM (2005) The blood-brain barrier: bottleneck in brain drug development. *NeuroRx* 2:3–14

Peuchen S, Duchen MR, Clark JB (1996) Energy metabolism of adult astrocytes *in vitro*. *Neuroscience* 71:855–70

Rami A, Volkmann T, Winckler J (2001) Effective reduction of neuronal death by inhibiting gap junctional intercellular communication in a rodent model of global transient cerebral ischemia. *Exp Neurol* 170:297–304

Rawanduzy A, Hansen A, Hansen TW, Nedergaard M (1997) Effective reduction of infarct volume by gap junction blockade in a rodent model of stroke. *J Neurosurg* 87:916–20

Saez JC, Contreras JE, Bukauskas FF, Retamal MA, Bennett MV (2003) Gap junction hemichannels in astrocytes of the CNS. *Acta Physiol Scand* 179:9–22

Schwartz JP, Nishiyama N, Wilson D, Taniwaki T (1994) Receptor-mediated regulation of neuropeptide gene expression in astrocytes. *Glia* 11:185–90

Sheikov N, McDannold N, Sharma S, Hynynen K (2008) Effect of focused ultrasound applied with an ultrasound contrast agent on the tight junctional integrity of the brain microvascular endothelium. *Ultrasound Med Biol* 34:1093–104

Sohl G, Maxeiner S, Willecke K (2005) Expression and functions of neuronal gap junctions. *Nat Rev Neurosci* 6:191–200

Toyofuku T, Yabuki M, Otsu K, Kuzuya T, Hori M, Tada M (1998) Direct association of the gap junction protein connexin-43 with ZO-1 in cardiac myocytes. *J Biol Chem* 273:12725–31

Treat LH, McDannold N, Vykhodtseva N, Zhang Y, Tam K, Hynynen K (2007) Targeted delivery of doxorubicin to the rat brain at therapeutic levels using MRI-guided focused ultrasound. *Int J Cancer* 121:901–7

Wallraff A, Kohling R, Heinemann U, Theis M, Willecke K, Steinhauser C (2006) The impact of astrocytic gap junctional coupling on potassium buffering in the hippocampus. *J Neurosci* 26:5438–47

Yamamoto T, Ochalski A, Hertzberg EL, Nagy JI (1990) LM and EM immunolocalization of the gap junctional protein connexin 43 in rat brain. *Brain Res* 508:313–9

Supplementary Information accompanies the paper on the Journal of Cerebral Blood Flow and Metabolism website (http://www.nature.com/jcbfm)